

Adaptive optics two photon scanning laser fluorescence microscopy

Yaopeng Zhou¹, Thomas Bifano² and Charles Lin³

1. In Vitro Imaging System, Abbott laboratories, 2 Research Way, 3rd Floor, Princeton, NJ 08540

2. Room 936, 8 Saint Mary's Street, Boston, MA 02215

3. Wellman Center for Photomedicine, Dermatology 185 Cambridge Street, Boston, MA 02114

Abstract

Two-photon fluorescence microscopy provides a powerful tool for deep tissue imaging. However, optical aberrations from illumination beam path limit imaging depth and resolution. Adaptive Optics (AO) is found to be useful to compensate for optical aberrations and improve image resolution and contrast from two-photon excitation. We have developed an AO system relying on a MEMS Deformable Mirror (DM) to compensate the optical aberrations in a two-photon scanning laser fluorescence microscope. The AO system utilized a Zernike polynomial based stochastic parallel gradient descent (SPGD) algorithm to optimize the DM shape for wavefront correction. The developed microscope is applied for subsurface imaging of mouse bone marrow. It was demonstrated that AO allows 80% increase in fluorescence signal intensity from bone cavities 145 μ m below the surface. The AO-enhanced microscope provides cellular level images of mouse bone marrow at depths exceeding those achievable without AO.

Key words: Adaptive optics, Two-photon and Zernike polynomial

1. Introduction

Two-photon fluorescence microscopy (TPFM) has been widely used for deep tissue imaging. Its unique ability of seeing through the tissue surface layers allows researchers to acquire high-resolution images of cell level details up to a few millimeters below the tissue surface. Various biological tissue, such as, brain[1], heart[2], kidney[3] and skin[4] have been studied by imaging with TPFM. We have developed a TPFM system with adaptive optics (AO) to study the stem cells and microenvironment in the bone marrow of mouse skull.

Hematopoietic stem cells (HSCs) resident in bone marrow and are responsible to maintain all cells found in blood (white blood cells, red blood cells and platelets) and immune system (B Cells, T cells, NK cells and dendritic cells) [5]. HSCs and their clinical applications have been widely studied. The medical application of adult stem cells has been exploited in existing treatments. For example, bone marrow

transplantation is routinely used in stem cell proliferation disorders, such as, leukemia, lymphomas and multiple myeloma.

It is desired to understand biological functionality of HSCs and the surrounding microenvironment in the bone marrow through *in vivo* imaging. However, both the imaging depth and imaging resolution are limited by tissue introduced optical aberrations in a conventional TPFM. With AO, we demonstrated improved imaging depth and resolution from optical aberration correction.

2. Methods

Zernike based stochastic parallel gradient descent algorithm

Conventional AO employs a sensor, such as the Shack-Hartmann wavefront sensor, to measure wavefront errors in the image-path of the optical system. These measured wavefront errors can be used as feedback to the wavefront corrector in a closed control loop that compensates for aberrations. However, in the TPFM, to improve photon collection efficiency, the fluorescence photons are collected by photon detectors right after the fluorescence photon exiting from the microscopic objectives. More importantly, the fluorescence light contains different optical aberrations due to the wavelength difference between the fluorescence light and the illumination light, which make it not useful in illumination light AO correction. Conventional wavefront sensing presents a much more complicated challenge in the TPFM setup. This is a fundamental problem for AO control, which generally requires some measured or modeled wavefront distortion data as a basis for compensation.

One alternative is to use a scalar measure of signal intensity (i.e., the metric) as the controller feedback signal. In this approach, the control objective is set to maximize fluorescence intensity by arbitrarily perturbing the multiple-degree-of-freedom of the deformable mirror. Some states of the mirror will produce larger intensity metrics than others. Through successfully perturbation, the metric can be optimized. The approach, known as sensor-less adaptive optics, is inefficient in comparison to conventional AO, but has proven to be effective for complex AO applications in which wavefront sensors are impractical [6,7].

The stochastic parallel gradient descent (SPGD) algorithm maximizes or minimizes a metric signal corresponding to system performance in an iterative control loop based on randomized perturbations of the system's controllable inputs. The control loop for AO includes temporarily changing the mirror shape by applying perturbations on its independent control inputs (e.g., DM actuators), assessing the effect of these perturbations on the metric (e.g., fluorescence intensity), estimating a metric gradient with respect to control input perturbations, and finally updating the mirror shape to a

state that should incrementally increase the metric. A block diagram is shown in the Figure 1. First, the current deflection state of each input channel of the deformable mirror is perturbed by a unit amount, in a direction that is randomly signed for each input channel. Note that the obvious basis for input to the DM is the DM actuators, with each actuator's input serving as an independent control channel. Other basis sets can be established as well. For example, one could control the DM based on basis sets coordinated over all actuators, with independent inputs corresponding to Zernike modes. The fluorescence signal is measured and stored as the metric value. Then the control channels are then perturbed in the opposite direction, and the metric is recorded again. The difference in recorded metric for positive and negative perturbations provides a gradient in the multidimensional input basis space, and a new state for the deformable mirror is determined by multiplying each input channel's signed perturbation by the global gradient and by adding this value to the previous input channel state. When the measured metric reaches a steady state, the loop is stopped.

The SPGD algorithm for AO in an actual fluorescence microscopy experiment in deep tissue imaging performs best when the control basis was Zernike polynomials, up to the 7th order, with perturbations applied as changes in the Zernike polynomial coefficients. Key factors in the effectiveness of the Zernike control basis in this SPGD application were that the Zernike polynomials closely approximate the expected aberrations in the microscope, and the Zernike based controller required fewer control degrees of freedom. In order to represent Zernike polynomial shape on the DM accurately, it is also necessary to drive each actuator precisely for the desired deflection profile. This is nontrivial, since the fundamental electrostatic actuation mechanism is nonlinear. In the previous publication [8], we introduced the calibration procedure for the MEMS DM (Boston Micromachines, MA) used in this work.

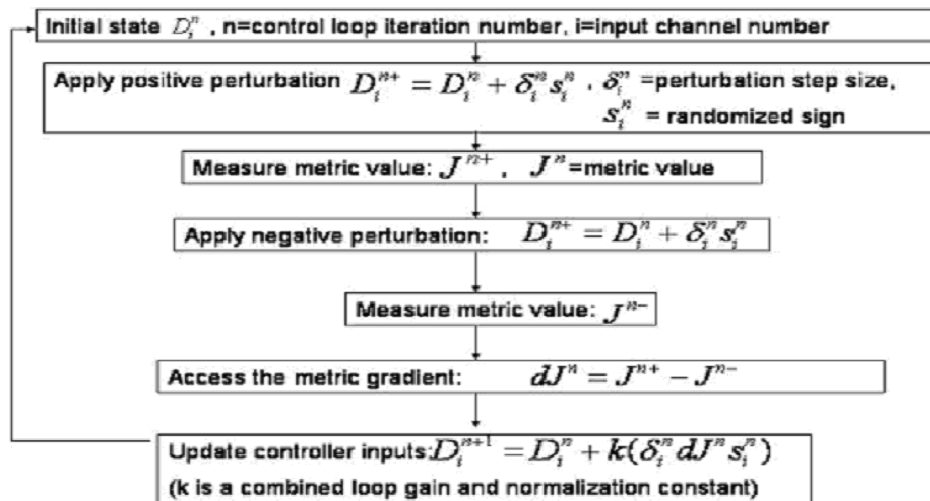


Figure 1. The flow chart of stochastic parallel gradient descent algorithm.

In the practical application of Zernike based SPGD algorithm for wavefront correction, we divide the first 35 Zernike terms into 3 different categories based on their order in the ANSI standard: Zernike term No. 3 to No.9 are in the first category, which are the 2nd and 3rd orders of Zernike polynomials. Piston, tip and tilt terms are ignored in the closed loop control. The second category includes Zernike term No. 10 to No. 20, which are the 4th and 5th orders of Zernike polynomials. The third category includes Zernike term No. 21 to No. 35, which are the 6th and 7th orders of Zernike polynomials.

These partitions are not entirely arbitrary. In the first group, there are the low order aberrations that dominate many optical microscopy systems, including astigmatism and coma. In the second group, there is the 1st order spherical aberration term that is expected to be particularly relevant to subsurface imaging. In the third group, there are higher order aberrations, including 2nd order spherical aberration, that define the highest relevant spatial frequency that are controllable with the MEMS DM.

Optical setup

The optical layout of the two-photon fluorescence microscope with adaptive optics is shown in Figure 2. The apparatus includes four main components: light source, wavefront correction, raster scanning and light detection.

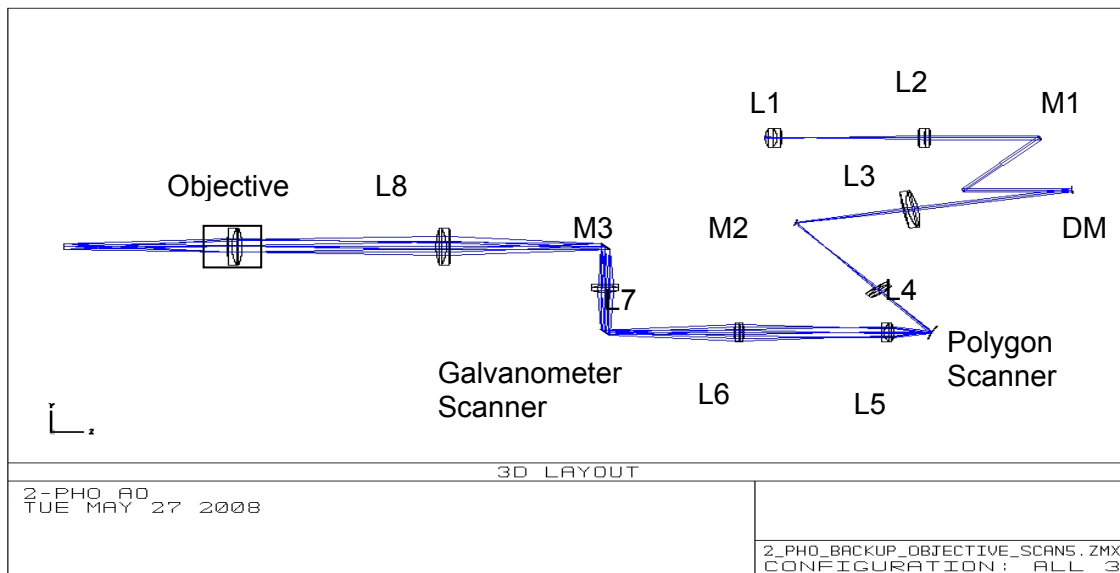


Figure 2. Optical layout of the two-photon fluorescence microscope with adaptive optics. L1-8: lens, M1-3: mirrors, DM: deformable mirror. L1 and L2 work as the collimator to expand the laser light. L3 and L4 work as relay lens to image the DM pupil onto the horizontal scanner (polygon scanner). L5 and L6 work as relay lens to image the polygon scanner onto the galvanometer scanner. L7 and L8 work as relay lens to image galvanometer scanner onto the back aperture of the imaging objective.

Light is delivered from a solid state mode-locked Ti-sapphire laser and an optical parametric oscillator (OPO) with combined tuning range from 700nm to 1300nm (Newport Corp., Irvine, CA). A pair of linear rotatable polarizers was installed to perform beam intensity control at the output of the laser.

The entrance pupil is defined by the MEMS DM. The MEMS DM has clear aperture of 4.8 X 4.8 mm occupied by the 12 X 12 actuator array. In order to create precise Zernike term shapes, the 10X10 actuator array is chosen to be the active area that defines the pupil. The entrance pupil is 4X4 mm.

The XY scanner is constructed using a polygon scanner (Lincoln Laser, AZ) and galvanometer scanner (Cambridge Technology, MA). The scanning system scans the focused beam across the specimen in a raster pattern. The polygon, capable of delivering constant scanning speed over a 20 degree optical angle, is in charge of the horizontal scan (fast scan). On the other hand, the galvanometer has an adjustable scanning angle, which provides the vertical scan (slow scan). The slow scan angle is changed to match the fast scan in order to provide a squared field of illumination on the imaging samples. Both the horizontal scanner and the vertical scanner are optically conjugated to the entrance pupil. A frame grab board is synchronized to the scanning mirrors, and is capable of grabbing up to 30 frames per second via a Macintosh computer (Apple, CA).

A photonmultiplier tube (PMT, Hamamatsu, Japan) is used for signal detection. The fluorescence signal is collected in a "non-descanned" fashion to maximize the detection of the scattered signal from the focal volume. The detector has a 3X12 mm active area, which requires focusing optics in the detection channel.

3. Results

The chosen imaging samples are genetically modified mice whose osteoplast express green fluorescent protein (GFP). The test mouse is anesthetized by injection of 80mg/kg Ketamine + 12 mg/kg Xylazine. The hair on the dorsal scalp is removed by applying a small quantity of hair remover cream, letting it work for 10 -15 minutes, followed by gently wiping off the area with a cotton swab. The area was then cleansed with sterile phosphate-buffered saline (PBS), disinfected by Betadine solution, followed by an excision of some of the skin covering the area. The imaging gel (Methocel 2%) was applied to the exposed area, and covered by the class-1 cover glass (Fisher Scientific, PA). All protocols were approved by the Subcommittee on Research Animal Care Application from Massachusetts General Hospital and performed by the researcher from the Wellman Center for Photomedicine.

The next two figures show the AO correction results at 145 μ m and 184 μ m below the surface. In order to avoid the focus shift caused by the defocus term created on the DM,

the focus term (Zernike term No. 4) is not adjusted during the closed loop SPGD correction. The images with AO on at both locations clearly show brighter features and sharper contrast.

AO correction at 145 μm below surface

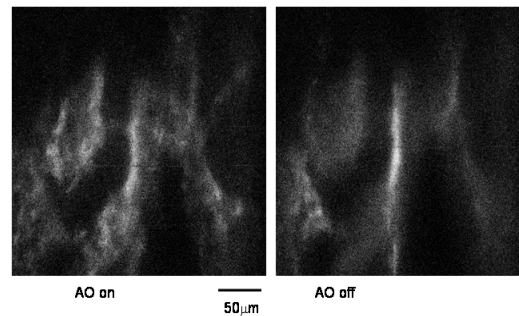


Figure 3. The bone cavities image with AO on/off at 145 μm below the surface.

AO correction at 184 μm below surface

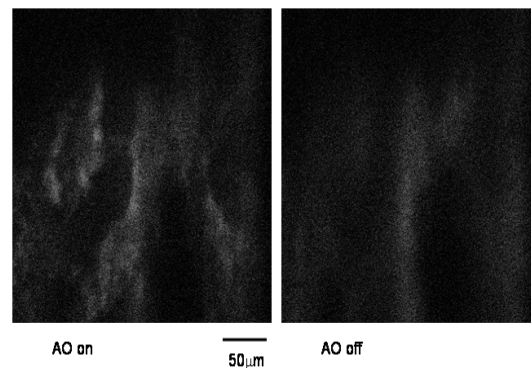


Figure 4. The bone cavities image with AO on/off at 184 μm below the surface.

Figure 5 shows a plot of the average intensity over the whole image frame measured every micrometer over a 200 μm imaging depth from the surface in the skull bone. The three data set correspond to conditions when the DM was held in its initial flat shape, when the DM was corrected using AO at an imaging depth of 145 μm , and when the DM was corrected using AO at an imaging depth of 184 μm . The intensity plot shows the improvements of intensity at the optimized locations, as well as the neighboring depth. For example, the intensity for the data set corrected at 145 μm depth is larger at 145 μm depth than the other two data sets, It is also notable that the two intensity plots with AO on showed weaker intensity at shallow depths (e.g., 0 to 120 μm). This is because the

DM shapes corrected at depths of 145 μm and 184 μm create optical aberrations in the shallow depth.

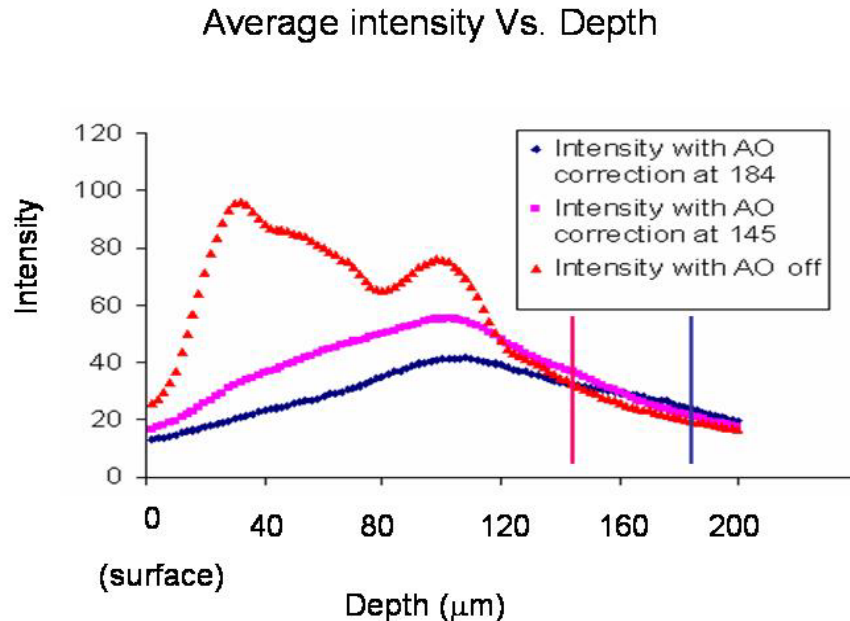


Figure 5. The average intensity plot of the non-linear signal at different depths with AO on/off.

If the images taken from 145 μm below the surface are used as the basis for quantified analysis, the average pixel value increases to 36.74 with AO on from 32.80 with AO off. However, if only the pixels that are larger than 100 (gray scale) are counted in the image with AO on, which roughly represent the fluorescence signal from the GFP, the average pixel value jumps to 130.50 with AO on from 72.12 with AO off. This represents an 81% increment in terms of intensity.

4. Conclusion

A system for the TPFM with AO has been designed, constructed and tested. The developed instrument includes a Ti-sapphire pulsed laser, a MEMS DM, a raster scanning system and a PMT as core components. The results have demonstrated the ability of deep tissue imaging in the mouse skull bone. AO is used to correct optical aberration for extending the imaging depth, as well as improving the image resolution and contrast. A sensor-less AO technique, namely a stochastic parallel gradient decent algorithm, is used with fluorescence intensity as a feedback signal to drive the DM in a way that compensates optical aberrations. To improve the AO loop efficiency for single-

input-multi-output system, a Zernike polynomial basis is used to control the DM. The Zernike polynomial based AO can compensate optical aberrations, and enhance the microscope's performance.

AO was applied to deep imaging of mouse skull tissue in genetically modified GFP mouse. The bone cavity structure was clearly resolved with AO at depth of 184 μ m. *In vivo* imaging of mouse bone marrow allows the study of the biological functionality of the HSCs and the surrounding microenvironment.

- [1] Winfried Denk and Karel Svoboda, "Photon Upmanship: Why Multiphoton Imaging Is More than a Gimmick", *Neuron*, Vol. 18, 351–357, March, 1997.
- [2] Rubart, M, "Two-photon microscopy of cells and tissue", *Circ. Res.* 95, 1154-1166 (2004).
- [3] Molitoris, B.A. and Sandoval, R.M., "intravital multiphoton microscopy of dynamic renal processes", *Am. J. physiol. Renal Physiol.* 288, F1084-F1089 (2005).
- [4] Laiho, L.H., Pelet, S., Hancewicz, T.M., Kaplan, P.D. and So, P.T., "Two-photon 3-D mapping of *ex vivo* human skin endogenous fluorescence species based on fluorescence emission spectra. *J. Biomed. Opt.* 10, 024016 (2005).
- [5] Cristina Lo Celso, Juwelle W. Wu, and Charles P. Lin, "*In vivo* imaging of hematopoietic stem cells and their microenvironment", *J. Biophoton.* 2, No. 11, 619–631 (2009).
- [6] Vorontsov, M.A. & Sivokon, V.P. "Stochastic parallel-gradient-descent technique for high-resolution wave-front phase-distortion correction." *Journal of the Optical Society of America, A*, 15 (10), 1998.
- [7] Wright, A.J. Burns, D., Patterson, B.A., Poland, S.P., Valentine, G.J. & Girkin, J.M.. Exploration of the Optimisation Algorithms Used in the Implementation of Adaptive Optics in Confocal and Multiphoton Microscopy. *Microscopy Research and Technique*, 67: 36-44, 2005.
- [8] Zhou, Y., and Bifano, T., "Characterization of contour shapes achievable with a MEMS deformable mirror", *Proc. SPIE Vol.* 6113, p. 123-130, 2006.